Journal of Structural Geology, Vol. 8, Nos. 3/4, pp. 291 to 304, 1986
Printed in Great Britain

0191-8141/86 $03.00 + 0.00
Pergamon Press Ltd.

Energy balance and deformation mechanisms of duplexes

GAUTAM MITRA

Department of Geological Sciences, University of Rochester, Rochester, NY 14627, U.S.A.

and

STEVEN E. BOYER

Sohio Petroleum Company, Technology Center, 5400 LBJ Freeway, Suite 1200, Dallas, TX 74240, U.S.A.

(*Received* 1 *July* 1984; *accepted in revised form* 29 *August* 1985)

Abstract—A duplex consists of a series of imbricate faults that are asymptotic to a roof thrust and a floor thrust. Depending on the final orientations of the imbricate faults and the final position of the branch lines, a duplex may be hinterland-dipping, foreland-dipping, or an antiformal stack. The exact geometry depends on various factors such as the initial dimensions of the individual slices (horses), their lithology, the amount of displacement (normalized to size of horse) on each fault, and the mechanics of movement along each fault.

The energy required in duplex formation can be determined by calculating the total work involved in emplacing each horse; this is given by

$$W_t = W_p + W_b + W_g + W_i,$$

where W_p is the work involved in initiating and propagating a fracture, W_b is the work involved in basal sliding, which may be frictional or some form of ductile flow, W_g is the work done against gravity during the emplacement of the horse, and W_i is the work involved in the internal deformation of the horse.

By calculating and comparing these work terms it is possible to predict the conditions under which the different types of duplexes will form. Normally, the development of a hinterland-dipping duplex is most likely. However, if deformation conditions are favorable, displacements on individual imbricate faults may be very large compared to the size of the horses, leading to the formation of either antiformal stacks or foreland-dipping duplexes.

INTRODUCTION

A DUPLEX fault zone consists of two parallel thrust faults (the roof and floor thrusts) bounding a family of subsidiary contraction faults which curve asymptotically into the roof and floor thrusts. Alternatively, a duplex may be defined as an imbricate family of horses (Boyer & Elliott 1982). Duplexes have characteristic internal features (Fig. 1): (1) beds within each horse trace out an elongate antiform–synform pair; (2) bedding near the inflection point within each horse is parallel to the sidiary faults; (3) bedding above and below the duplex is relatively undisturbed and (4) for long distances the same stratigraphic horizon may compose the hanging-wall of the roof thrust or the footwall of the floor thrust.

A duplex fault zone forms by sequential imbrication in the direction of tectonic transport (Boyer 1978, Boyer & Elliott 1982, fig. 19). Each imbricate fault branches from the floor fault along a trailing branch line and rejoins the roof fault along a leading branch line (Boyer & Elliott 1982, Hossack 1983) (Fig. 1). As each new imbricate fault forms, the previous imbricate fault is deactivated

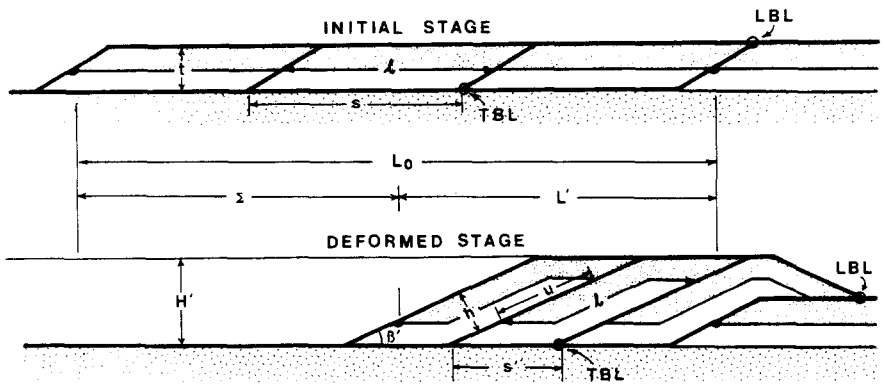

Fig. 1. Initial and deformed stages in formation of a duplex (modified after Boyer & Elliott 1882). Dimensions shown are initial length (ℓ) and stratigraphic thickness (t) within each horse, initial fault spacing s, initial duplex length L_0, deformed duplex length L', shortening distance Σ, structural thickness H', final angle between floor fault and imbricates, (β'), final fault spacing s', and displacement on each fault (u). Also shown are the trailing branch line (TBL) and the leading branch line (LBL) for the last horse before and after motion on the last thrust.

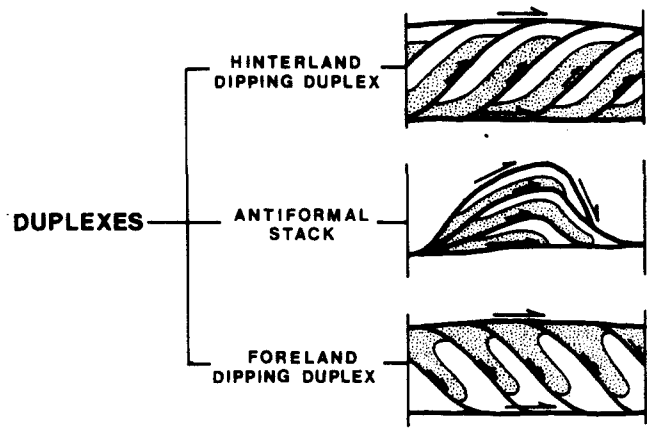

Fig. 2. Classification of different types of duplexes (modified after Boyer & Elliott 1982).

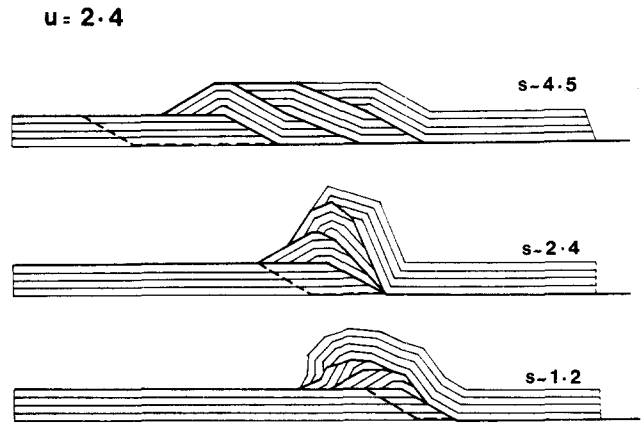

Fig. 3. Change in duplex geometry with initial fault spacing, keeping displacements on individual faults constant. s is the initial spacing between imbricate faults, and u is the displacement on each fault.

and carried passively with the enclosing thrust sheet. The imbricate faults transfer slip away from a stratigraphically lower glide horizon to a stratigraphically higher glide horizon. Displacement on each subsidiary (imbricate) thrust is minor compared to that on the roof and floor thrusts. These displacements move the branch lines closer together during formation of a typical hinterland-dipping duplex (Fig. 2). If displacements on imbricate thrusts are large enough, branch lines coincide or bunch up, and an antiformal stack is formed (Boyer & Elliott 1982). With even larger displacements on individual imbricate thrusts, each branch line passes over and beyond the underlying one, producing a foreland-dipping duplex (Boyer & Elliott 1982).

Details of the dimensions and internal geometry of duplexes have been previously discussed by Boyer & Elliott (1982), who derived relationships (Boyer & Elliott 1982, eqs 1–8) between initial (L_o) and current (L') duplex length, shortening distance (Σ), structural thickness (H'), cross-section area (A), initial stratigraphic thickness within each horse (t), bed length within each horse (ℓ), current angle between floor fault and imbricate faults (β'), current perpendicular distance between imbricate faults (h'), and current spacing between imbricate faults measured parallel to the floor thrust (s') (Fig. 1). If we denote the initial spacing between the imbricate faults, measured parallel to the floor thrust, as s, and the displacement on each imbricate fault as u (Fig. 1), we can describe some additional geometric characteristics of duplexes.

For $u < s$, the duplex is hinterland dipping.

For $u = s$, the structure is an antiformal stack.

For $u > s$, the duplex is foreland dipping.

Thus there is a continuous transition between the different types of duplexes depending on the relative magnitudes of fault spacing and displacements on individual faults.

If the displacement on individual imbricate faults is held constant, then it can be shown by simple geometric construction (Fig. 3) that decreasing fault spacing (i.e. shorter imbricate slices) will result in a change from a hinterland-dipping duplex to an antiformal stack, and finally to a foreland-dipping duplex.

If on the other hand, initial spacing between imbricate faults is held constant (i.e. imbricate slices of constant size), then increasing displacement on individual faults will result in transition from a hinterland-dipping duplex to an antiformal stack, and finally to a foreland-dipping duplex (Fig. 4). An ideal foreland-dipping duplex with parallel roof and floor thrusts is produced when the displacement is twice the initial fault spacing.

Under natural conditions of deformation, neither fault spacing nor displacement on individual faults remains constant throughout a duplex. Relative magnitudes of fault spacing (s) and displacement (u) may change along strike resulting in change from a hinterland-dipping duplex to an antiformal stack as in the

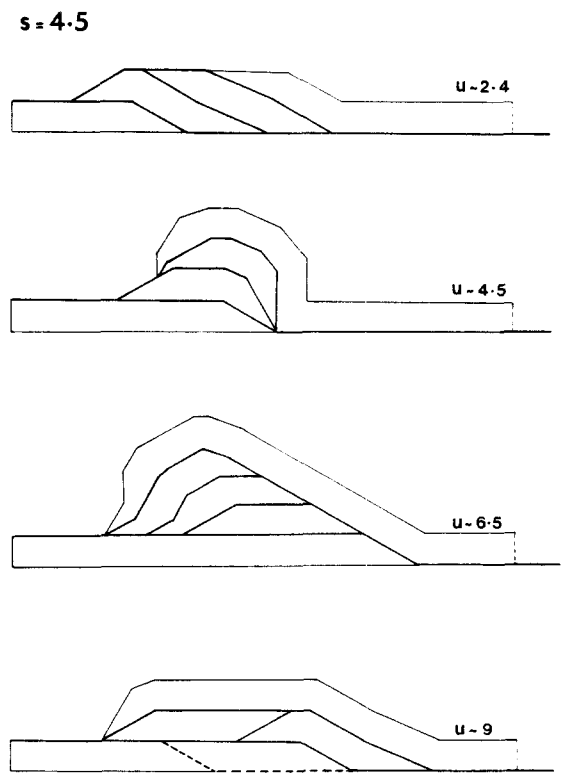

Fig. 4. Change in duplex geometry with variation in displacement on individual faults, keeping initial spacing between faults constant. s is the initial spacing between imbricate faults, and u is the displacement on each fault.

footwall of the Moine thrust (Elliott & Johnson 1980, figs. 4, 12, 18 and 24, Boyer & Elliott 1982, figs. 14 and 23) and the footwall of the Ben More thrust (Coward 1984, fig. 3). If the changes in relative magnitude of spacing (s) and displacement (u) are even larger, it may result in a transition from a hinterland-dipping duplex to a foreland-dipping duplex as in the Mountain City window in Tennessee (Boyer & Elliott 1982, Diegel 1986) (Fig. 5a). Fault spacing (s) and displacement (u) may also change during progressive development of a duplex. If u/s decreases, the duplex may show continuous transition from an antiformal stack to a hinterland-dipping duplex as in the forward part of the Haig Brook duplex (Fermor & Price 1976) (Fig. 5c); or a folded duplex formed by some other means (e.g. a blind imbricate complex underneath) may lose its folding as the duplex continues to develop, as in the forward part of the Mt. Crandell duplex (Boyer & Elliott 1982) (Fig. 5b). If u/s increases during duplex development, the duplex structure may change from a hinterland-dipping duplex to an antiformal stack as in the middle part of the Haig Brook duplex (Fig. 5c), or even to a foreland-dipping duplex as in the southern part of the Mountain City window duplex (Diegel 1986) (Fig. 5a).

The spacing between imbricate faults (s) and the displacement on each fault (u) depend on the mechanics of fault growth and fault motion, and are determined by the relative energy requirements for these processes. These energy requirements and other energy terms important in duplex growth will now be discussed.

MECHANICS OF DUPLEX DEVELOPMENT

Gretener (1972) suggested that thrust faulting is a self-perpetuating process; the emplacement of one thrust sheet sets up conditions that favor the initiation of a new thrust fault. This concept applies to the formation of duplex imbricates as well. Once a duplex zone is initiated, the duplex will advance and grow until the deforming stresses are removed or become too weak to induce movement.

Why does a duplex zone develop in some situations, when a single fault may account for all the slip in other situations? The answer probably lies in the mechanics of fault motion. A fault zone in a weak glide horizon can accommodate large strains at constant low stresses. Thus, very large displacements can be achieved along fairly narrow fault zones (Schmid 1983, Mitra 1984). The glide horizon may be a lithologically weaker layer (e.g. shale, coal, salt). Alternatively, it may develop as a strain softening zone due to a change in the dominant deformation mechanism resulting from grainsize reduction during progressive deformation; this may be achieved under both ductile (Schmid 1983) and brittle (Mitra 1984) conditions, as long as the grainsize is reduced beyond a certain limit.

If a fault ramp forms, it does so by the fault climbing out of a glide horizon, through a more competent unit, into a higher glide horizon. While deformation within the glide horizon is ductile, deformation within the competent unit may be dominantly brittle. In this case grainsize reduction along the fault zone in the competent unit is controlled by the Hall–Petch relation (Mitra 1978), an inverse relationship between stress and grainsize. Thus, deformation along the fault zone in the competent unit may actually be a strain-hardening process, so that displacement along this zone becomes increasingly difficult with progressive strain. Eventually a second ramp fault forms, along which slip is transferred from the lower glide horizon to the higher glide horizon. Successive development of new ramp faults requires less energy than continued movement on a single, strain-hardening fault, and thus a duplex zone develops.

The conditions under which the different types of duplexes will evolve can be defined by evaluating the energy requirements for alternative paths during duplex development. Following the principle of minimum work (Nadai 1963), at each stage, the path which requires the least work will be the favored path. This principle assumes stable equilibrium, and can also be extended to problems involving quasi-static deformation where the system passes through a series of equilibrium states (Martin 1975). Most deformation at geologic strain-rates is essentially quasi-static, involving, for example, negligibly small radiational and inertial components (which we have ignored in our equations). Two special cases are useful to consider, namely the transition from hinterland-dipping duplex to antiformal stack, and the transition from antiformal stack to foreland-dipping duplex.

Case I: Transition from a hinterland-dipping duplex to an antiformal stack

Consider a duplex structure after the formation of three imbricate slices with $u < s$ (Fig. 6). Within the duplex the section has been doubled in the area overlying the footwall step. Continued movement can now occur

Fig. 5. Examples of changes in duplex geometry within thrust belts: (a) Mountain City window with the northern cross-section (AB) showing a hinterland-dipping duplex (after Boyer & Elliott 1982), and the southern cross-section (CD) showing a forward-dipping duplex (after Diegel 1986); both sections show approximately 15.7 km of total translation along imbricate faults. Section AB has a mean fault spacing ($\bar{s}$) of 4.8 km, mean fault translation ($\bar{u}$) of 2 km and mean u/s of 0.41. Section CD has $\bar{s}$ = 2.3 km, $\bar{u}$ = 2.6 km and mean u/s = 1.2. (b) Mount Crandell duplex (after Boyer & Elliott 1982) shows the development of an antiformally folded duplex due to large displacement of one small horse and the presence of an underlying blind imbricate complex. Folding is lost in the front of the duplex as fault spacing increases abruptly. (c) Haig Brook duplex (after Fermor & Price 1976) shows across strike change in geometry. Fault spacing is remarkably uniform, with a mean spacing of 85 m. The middle part shows change from a hinterland dipping duplex to an antiformal stack due to a sudden increase in displacement on faults (mean u/s changes from 0.7 to 1.2). The forward part of the duplex shows transition back to a hinterland dipping duplex, as fault spacing increases, and mean u/s decreases to 0.4.

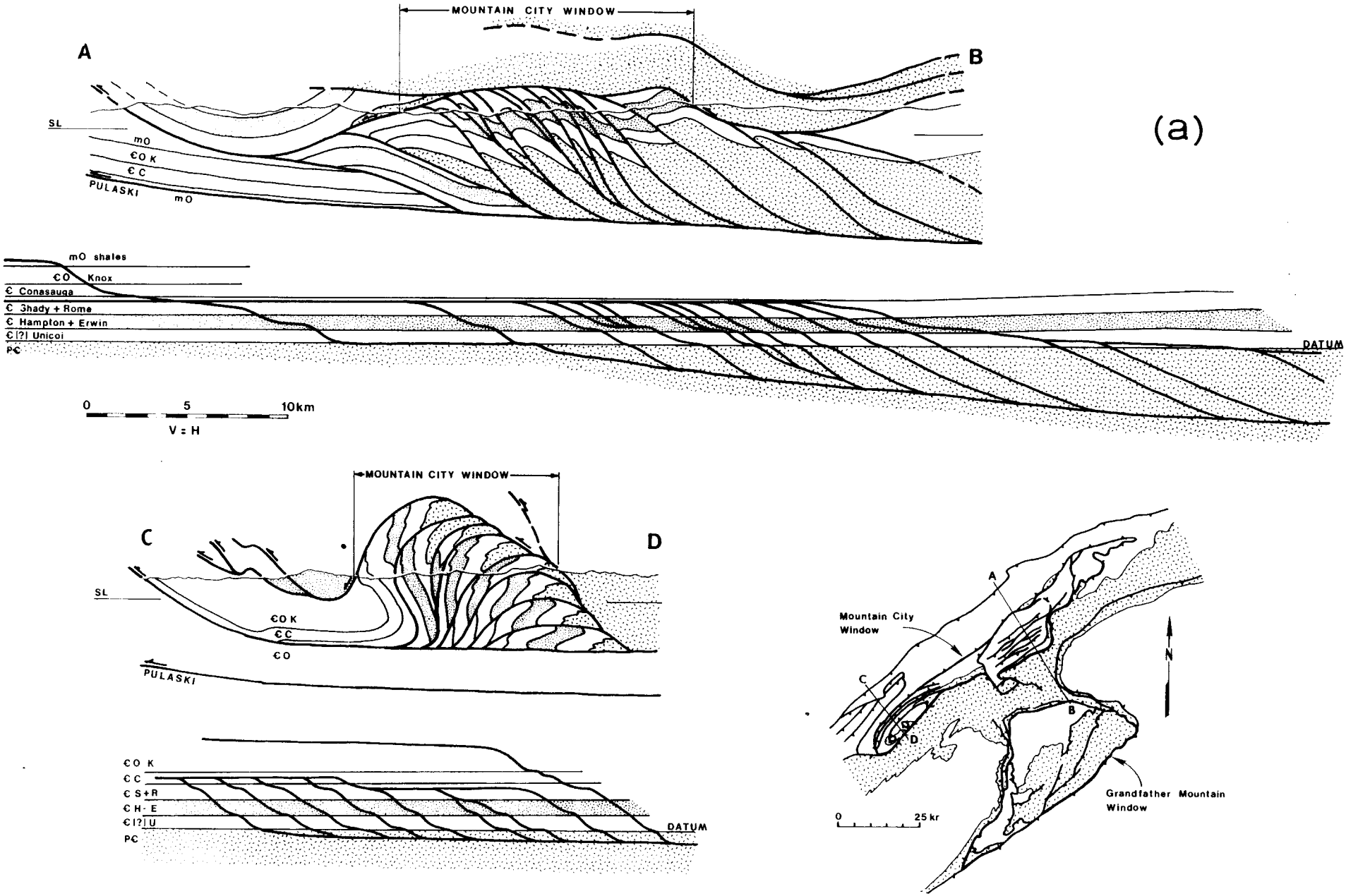
MOUNTAIN CITY WINDOW
A
B
SL
mO
€O K
€C
PULASKI
mO
(a)
mO shales
€O Knox
€ Conasauga
€ Shady + Rome
€ Hampton + Erwin
€ ?| Unicoi
P€
DATUM
0
5
10km
V = H
MOUNTAIN CITY WINDOW
C
D
SL
€O K
€C
€O
PULASKI
€O K
€C
€ S+R
€ H-E
€ ?| U
P€
DATUM
Mountain City Window
A
B
C
D
N
Grandfather Mountain Window
0
25 kr

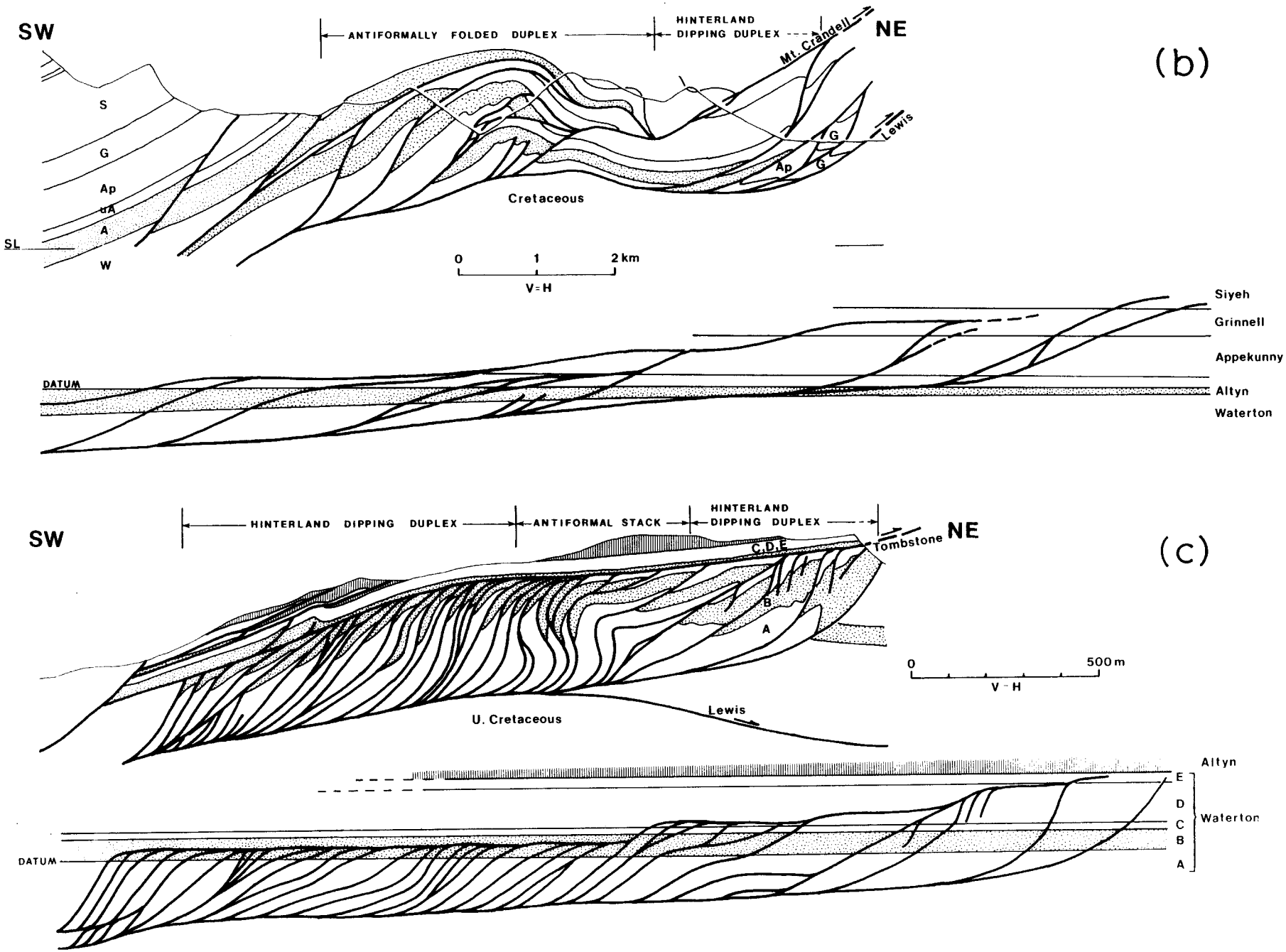
SW
ANTIFORMALLY FOLDED DUPLEX
HINTERLAND
DIPPING DUPLEX
NE
Mt. Crandell
Lewis
(b)
S
G
Ap
dA
A
W
SL
G
Ap
G
Cretaceous
0
1
2 km
V=H
Siyeh
Grinnell
Appekunny
Altyn
Waterton
DATUM
SW
HINTERLAND DIPPING DUPLEX
ANTIFORMAL STACK
HINTERLAND
DIPPING DUPLEX
NE
Tombstone
(c)
C,D,E
B
A
0
500 m
V = H
U. Cretaceous
Lewis
Altyn
E
D
C
B
A
Waterton
DATUM

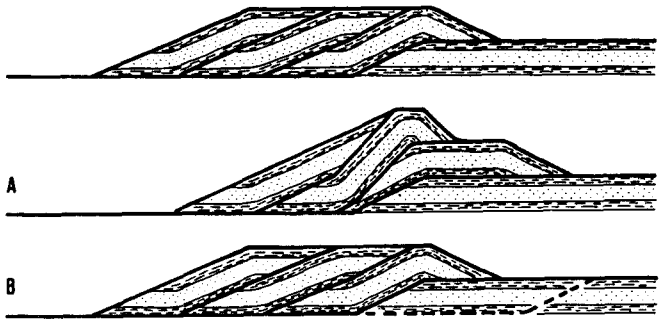

Fig. 6. Upper section shows a duplex with three imbricates. Continued movement may proceed by further displacement on the last formed imbricate (path A) or by formation of a new imbricate fault (path B).

along two different paths. Movement may proceed along the existing floor fault, resulting in the folding of earlier formed imbricates (path A). Or, a new fault may form at the base of the footwall step (path B). The path which is selected will be the one that involves the least expenditure of work. For the continued development of a hinterland-dipping duplex, path B is favored. If path A is favoured an antiformal stack develops.

The total work, W_t, performed in the development of a duplex fault structure can be subdivided into four parts.

$$W_t = W_p + W_b + W_g + W_i, \tag{1}$$

where W_p is the work performed in initiation and propagation of imbricate faults; W_b is the work needed to overcome resistance to sliding along the base of the faults; W_g is the work required to move the thrust masses up-section against the force of gravity and W_i is the work consumed in the internal deformation of the horses, which includes both folding within the sheet (W_k), as well as overall simple shear of the sheet (W_s), i.e. $W_i = W_k + W_s$.

We start with an imbricate structure made up of three slices (Fig. 7). An additional displacement, u, is added by two alternative paths: path A which involves continued movement on the last imbricate fault formed and resultant folding of pre-existing imbricate slices, or path B where movement is transferred to a new imbricate fault.

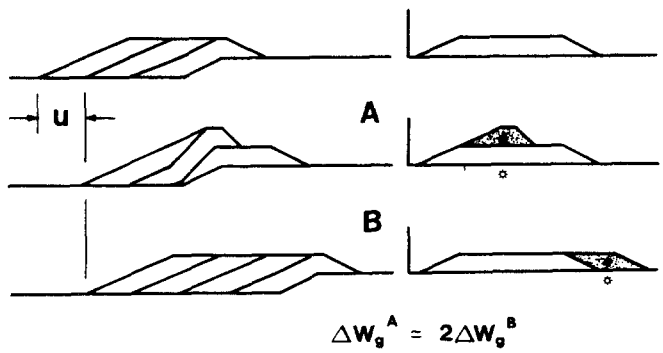

Fig. 7. Upper section shows a duplex with three imbricates. Additional displacement (u) is achieved by continued movement on last imbricate (path A) or by formation of and movement on a new imbricate (path B). Shaded portions of graphs at right represent cross-sectional area of the mass moved up-section against gravity; this area is raised twice as high in A as in B, indicating that twice as much gravitational work (ΔW_g) is performed. Open stars represent datum above which mass moved is raised. Distance between open and closed stars is the height through which mass is raised.

The total increment of work performed during displacement u is denoted by ΔW_t and will be calculated for a cross-sectional slice of unit width perpendicular to the

For path A no new thrust is created and propagated.

$$\Delta W_{p_A} = 0. \tag{2}$$

For path B work must be done so that a new thrust surface can initiate and propagate. In addition, a zone of cataclasite or mylonite develops along the fault zone; this grainsize reduction requires additional work to create the new surface area.

$$\Delta W_{p_B} = S_e \cdot p \cdot 1 + S_e \cdot A_v \cdot p \cdot a_c \cdot 1, \tag{3}$$

where S_e is the surface energy per unit area, p is the down-dip length of the fault, A_v is the new surface area per unit volume created in the rock during grainsize breakdown and a_c is the thickness of the cataclasite or mylonite zone.

Elliott (1976b) defined basal sliding work in such a way that it occurs only along the thrust, a two dimensional surface of zero thickness. It is given by

$$\Delta W_b = C \cdot \tau_b \cdot p \cdot u \cdot 1, \tag{4}$$

where C is an averaging factor which accounts for the amount of slip that may be added by simple shear as the thrust climbs section, τ_b is the basal shear stress and u is the displacement.

During the increment of movement, u is the same for both cases, and the fault lengths (p) are the same. Both C and τ_b may vary, but are approximately the same order of magnitude in the two cases, so

$$\Delta W_{b_A} \simeq \Delta W_{b_B}. \tag{5}$$

Work performed against gravity can be calculated by observing the change in mass above a given datum (Fig. 7). The reference line was chosen to be the top of the thrust faulted section prior to the increment of deformation. The right hand side of the diagram (Fig. 7) shows the cross-sectional area of the total material moved against gravity; only the mass within the duplex is considered. After an increment of displacement, u, the material above the datum has been increased by the amount shown by the stippled area. The amount of work performed against gravity during this increment is given by

$$\Delta W_g = \rho \cdot A \cdot h \cdot g \cdot 1, \tag{6}$$

where ρ is the rock density, A is the cross-sectional area, h is the height through which the mass is raised and g is gravitational acceleration. Since displacement is the same for paths A and B, the cross-sectional area, and thus the mass of material added, is the same for paths A and B (Fig. 7). The height through which the mass is raised can be measured in terms of the vertical distance between two horizons that were at the same level before faulting (distance between open and closed stars). It is found that

$$h_B \simeq \tfrac{1}{2} h_A \tag{7}$$

and

$$\Delta W_{g_A} \simeq 2\,\Delta W_{g_B}. \tag{8}$$

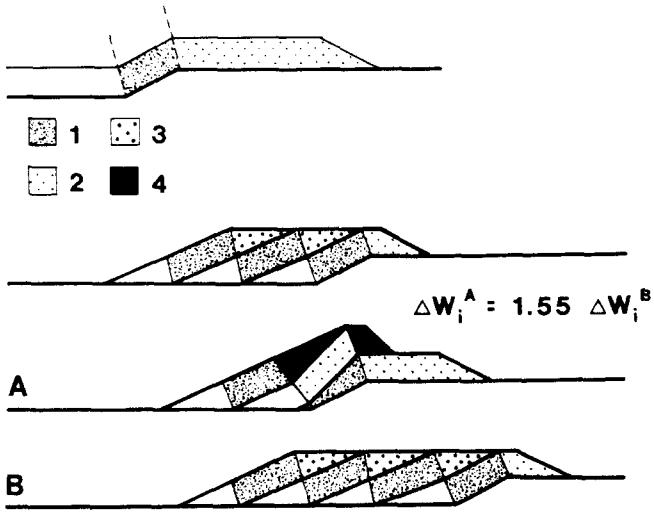

Fig. 8. Approximation of the internal work by kinking for path A and path B. Rocks of the hangingwall pass through a standing kink band at the footwall ramp (as shown in upper left inset). The number of the kink planes that a body of rock has passed through is indicated by shading. More work is involved in path A than path B. See text for discussion.

Less easily estimated is the work (W_i) expended in internal deformation of the horses. As a first approximation this can be subdivided into work due to kinking within the sheet, and work due to simple shear of the sheet as a whole. A rough estimate can be made of the kinking work in the following way. In each case the thrust mass is divided into subareas based on the number of kink planes a given volume of rock passes through (Fig. 8). In a simple thrust sheet there is one kink plane at the base of the footwall step and one at the top of the step. These kink planes set up a standing wave through which rocks of the hanging wall pass. In the area of the footwall step the work done in kinking any horse is given by (see Appendix)

$$\Delta W_k = \tau_{12} \cdot \sum_{i=1}^{n} \left(A_i \cdot \sum_{j=1}^{p} \tan \theta_j \right), \tag{9}$$

where τ_{12} is the interbed shear stress, n is the number of subareas into which the horse is subdivided, a_i is the cross-sectional area of each subarea, p is the number of kink planes each body of rock has passed through and θ_j is the angle through which the rocks have been kinked. For the entire duplex, made up of m horses, the work done in kinking is given by (see Appendix)

$$W_k = \sum_{1}^{m} \left[\tau_{12} \cdot \sum_{i=1}^{n} \left(A_i \cdot \sum_{j=1}^{p} \tan \theta_j \right) \right]. \tag{10}$$

Calculating the work for path A and path B, it was found that

$$W_{k_A} \simeq 1.55 W_{k_B}. \tag{11}$$

Equation (11) is probably an underestimate for W_{k_A} since path A probably involves significantly larger amounts of work. This is because the process of folding part of a pre-existing imbricate stack involves transferring slip between imbricate fault planes and the bedding planes within imbricate slices. This slip transfer is easier if bedding is perfectly parallel to the imbricate faults, but this is not the case in path A. Bedding within the individual imbricate slices is folded, so that it is locally parallel to the imbricate faults, but meets the imbricate faults at high angles in other places. Therefore, slip is not easily transferred from one imbricate fault to another, making continued movement on an existing fault easier than movement on a new one. It is reasonable to conclude that if we consider the average work per imbricate slice (ΔW_k) along the two paths,

$$\Delta W_{k_A} > \Delta W_{k_B}. \tag{12}$$

In addition to the folding of beds within each imbricate sheet, the rocks within each sheet undergo large amounts of simple shear deformation, particularly in a narrow zone close to the thrust plane. The motion of a thrust sheet deforming under brittle conditions (such as the Cumberland Plateau sheet in the Tennessee Appalachians, and the Copper Creek and Hunter Valley sheets east of the Pine Mountain Block in Virginia) can be shown to be approximately plastic (Wojtal 1982). Thrust sheets at much higher metamorphic grades are also emplaced as perfectly plastic sheets as shown by their deformation profiles. A sheet's deformation profile, in simplest terms, is described by the change in shape of a material line that started out being perpendicular to the thrust fault (Wojtal 1982). An excellent example is the Särv thrust sheet in the Swedish Caledonides where deformed dikes that were originally perpendicular to the thrust are now asymptotic to the thrust along a thin basal zone (Gilotti & Kumpulainen 1986). Deformation as a perfectly plastic sheet results in a very highly sheared basal layer, with an abrupt transition into an almost undeformed upper section. In a strain-hardening thrust sheet, the thickness of the basal sheared layer increases linearly with displacement under both brittle (Robertson 1982, 1983) and ductile (Mitra 1979) conditions; it is therefore possible to determine the shear strain (γ) if the displacement (u) is known.

The work done in shearing the basal layer is

$$W_s = \tau_b \cdot \gamma \cdot p \cdot t_b \cdot 1, \tag{13}$$

where γ is the shear strain given by

$$\gamma = \frac{u}{t_b} \tag{14}$$

and t_b is the thickness of the basal deformed zone. For path A, displacement continues along the same fault for two increments of motion, leading to a basal layer that is twice as thick as in path B.

$$\Delta W_{s_A} = \tau_b \cdot \frac{u}{2t_b} \cdot p \cdot 2t_b \cdot 1, \tag{15}$$

$$\Delta W_{s_B} = \tau_b \cdot \frac{u}{t_b} \cdot p \cdot t_b \cdot 1 \tag{16}$$

and

$$\Delta W_{s_A} = \Delta W_{s_B} \quad \text{for basal shearing.} \tag{17}$$

For continued imbrication to be favored, the total work in path B must be less than that in path A; that is,

$$(\Delta W_p + \Delta W_b + \Delta W_g + \Delta W_k + \Delta W_s)_B < (\Delta W_p + \Delta W_b + \Delta W_g + \Delta W_k + \Delta W_s)_A. \tag{18}$$

Substituting results obtained from equations (2), (5), (8) and (17), this condition simplifies to

$$\Delta W_{p_B} + \Delta W_{k_B} - \Delta W_{g_B} < \Delta W_{k_A} \tag{19}$$

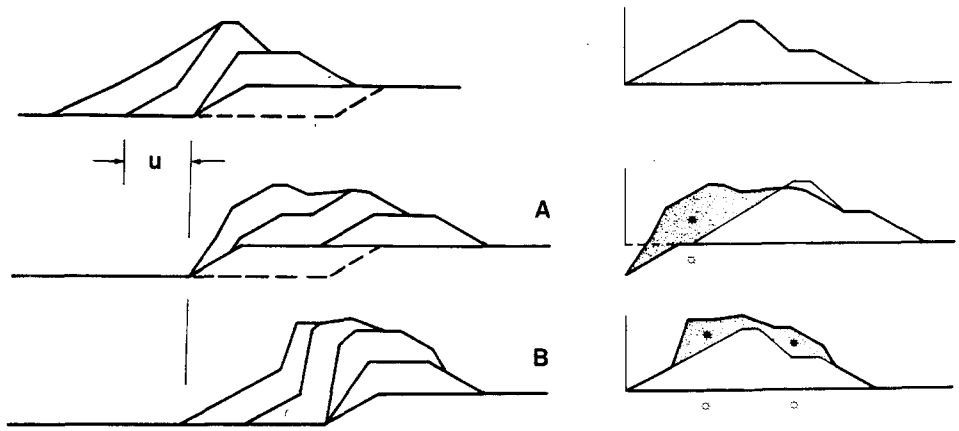

Fig. 9. Upper section shows a duplex with coinciding branch lines giving rise to an initial antiformal stack. Additional displacement (u) is achieved by continued movement on last imbricate (path A), or by formation of and movement on a new imbricate (path B). Shaded portions of graphs at right represent cross-sectional area of the mass moved up-section against gravity. Path B involves a larger amount of gravitational work. Open stars represent datum above which mass moved is raised. Distance between open and closed stars is the height through which mass is raised. See text for discussion.

or, for continued imbrication,

$$\frac{\Delta W_{p_B} - \Delta W_{g_B}}{\Delta W_{k_A} - \Delta W_{k_B}} < 1. \quad (20)$$

An antiformal stack would be favored if

$$\frac{\Delta W_{p_B} - \Delta W_{g_B}}{\Delta W_{k_A} - \Delta W_{k_B}} > 1. \quad (21)$$

Case II: Transition from an antiformal stack to a foreland-dipping duplex

Now consider a duplex structure after the formation of three horses, where the trailing branch line of the last-formed imbricate thrust coincides with the trailing branch line of the preceding thrust (i.e. $u = s$). Continued movement can again take place along two different paths.

Movement may continue along the existing fault plane, carrying the trailing branch line of the last-formed imbricate thrust over and beyond the trailing branch line of the next (future) thrust (path A). This would produce an ideal forward-dipping duplex (as shown by Boyer & Elliott 1982, fig. 24) only if the total displacement of the trailing branch line is twice the thrust spacing ($u = 2s$) i.e. $u = s$ for the increment of deformation we are considering here. Somewhat smaller displacements would also produce forward-dipping duplexes, but these would have some characteristics of an antiformal stack, with the roof thrust being convex with respect to a planar floor thrust.

The alternative to path A is the formation of a new fault at the base of the footwall step (path B). A displacement $u = s$ along this new fault would produce the same slip transfer from floor thrust to roof thrust as path A, but would result in further development of the antiformal stack that existed before this increment of deformation.

The favored path would be the one involving the least expenditure of work. The total increment of work performed during displacement u is denoted as before by ΔW_t, which (using eqn 1) is given by

$$\Delta W_t = \Delta W_p + \Delta W_b + \Delta W_g + \Delta W_i, \quad (22)$$

where the four parts are, work to initiate and propagate a fault (ΔW_p), work in basal sliding (ΔW_b), work against gravitational forces (ΔW_g), and work in internal deformation (ΔW_i) involving work due to folding (ΔW_k) and work due to simple shear of the sheet (ΔW_s). The increment of work (ΔW_t), for a cross-sectional slice of unit width perpendicular to the diagram, is calculated for the two possible paths.

For path A, no new thrust is created and propagated

$$\Delta W_{p_A} = 0. \quad (23)$$

For path B a new fault is formed, and the work needed for this is given, as before (eqn 3) by

$$\Delta W_{p_B} = S_c \cdot p \cdot 1 + S_c \cdot A_v \cdot p \cdot a \cdot 1, \quad (24)$$

where the first term on the right hand side is the work done in initiation and propagation of the new thrust surface, and the second term is the work done in developing the zone of cataclasite or mylonite that is produced along the thrust.

Basal sliding work is calculated as before (eqn 4) as the work due to sliding on a two-dimensional surface of zero thickness (Elliott 1976b). It is approximately the same for the two cases and is given by

$$\Delta W_{b_A} \simeq \Delta W_{b_B} = C \cdot \tau_b \cdot p \cdot u \cdot 1. \quad (25)$$

Work performed against gravity can be calculated by determining the change in mass above a datum (Fig. 9). The reference condition was chosen as the configuration before the last increment of deformation. The cross-sectional area of the total mass moved against gravity is shown in the right hand diagram (Fig. 9); only the mass within the duplex is considered. The geometry shown is constructed using a fault-bend fold model (Suppe 1983), but the complexity of the structure produced suggests that other configurations are possible depending on

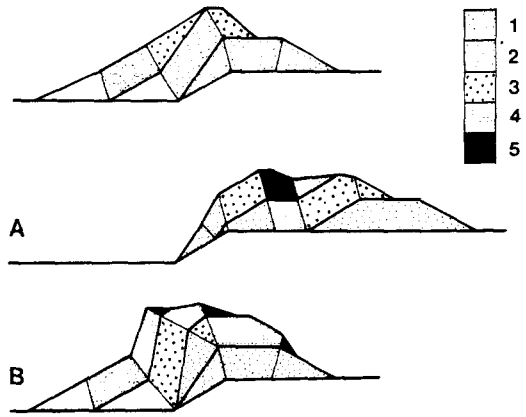

Fig. 10. Approximation of the internal work by kinking for path A and B. The number of kink planes a body of rock has passed through is indicated by shading. Path B involves more work. See text for discussion.

relative proportions of bedding-plane slip and fault-plane slip, and on how closely real structures follow kink geometries used in the fault-bend fold model. After the last increment of deformation, the material above the datum is increased by an amount shown by the stippled areas. The work performed against gravity during this increment is given by

$$\Delta W_g = \rho \cdot A \cdot h \cdot \boldsymbol{g} \cdot 1. \tag{26}$$

The added cross-sectional area in path B has an irregular shape, and has to be divided into subareas which have been raised through different heights.

$$\Delta W_{g_B} = \sum_{i=1}^{n} \rho \cdot A_i \cdot h_i \cdot \boldsymbol{g} \cdot 1. \tag{27}$$

It is found that

$$\Delta W_{g_B} \simeq 1.47\ \Delta W_{g_A}. \tag{28}$$

The work expended in internal deformation of the horses includes work involved in folding and simple shear of the sheet, and is quite difficult to determine in this case, because of the complicated folding that individual horses undergo along both paths. However, the folding work can be estimated by assuming kink geometries developed by fault-bend folding (Suppe 1983). In each case, the thrust mass is divided into subareas based on the number of kink planes a given volume of rock passes through (Fig. 10). For the entire duplex, the work done in kinking is given as before by

$$W_k = \sum_{1}^{m} \left[\tau_{12} \cdot \sum_{i=1}^{n} \left(A_i \cdot \sum_{j=1}^{p} \tan \theta_j \right) \right]. \tag{29}$$

It is found that in forming the entire duplex,

$$W_{k_B} = 1.16 W_{k_A}. \tag{30}$$

However, if we look at the deformation due to the last increment of displacement ($u = s$) that we are considering,

$$\Delta W_{k_B} = 1.42\ \Delta W_{k_A}. \tag{31}$$

The rocks within each imbricate sheet also undergo large amounts of simple shear deformation, particularly close to the thrust plane. The thickness of this basal deformed zone increases with displacement (Robertson 1983). The work done in shearing the basal layer is,

$$\Delta W_s = \tau_b \cdot \gamma \cdot p \cdot t_b \cdot 1, \tag{32}$$

where the shear strain is given by

$$\gamma = \frac{u}{t_b}. \tag{33}$$

As before (eqs 15 and 16), the thickness of the basal deformed zone in path A is twice that in path B because of the larger accumulated displacement along a single fault in path A. Hence, for the last increment of displacement that we are considering

$$\Delta W_{s_A} = \tau_b \cdot \frac{u}{2t_b} \cdot p \cdot 2t_b \cdot 1, \tag{34}$$

$$\Delta W_{s_B} = \tau_b \cdot \frac{u}{t_b} \cdot p \cdot t_b \cdot 1 \tag{35}$$

and

$$\Delta W_{s_A} = \Delta W_{s_B} \quad \text{for basal shearing.} \tag{36}$$

For continued imbrication, and hence stacking, to be favored the total work in path B must be less than that in path A; i.e.

$$(\Delta W_p + \Delta W_b + \Delta W_g + \Delta W_k + \Delta W_s)_B < (\Delta W_p + \Delta W_b + \Delta W_g + \Delta W_k + \Delta W_s)_A. \tag{37}$$

Substituting results obtained from eqs (23), (25), (28) and (36), this condition simplifies to

$$\Delta W_{p_B} + \Delta W_{k_B} < \Delta W_{k_A} - 0.5\ \Delta W_{g_A} \tag{38}$$

or

$$\frac{\Delta W_{p_B} + \Delta W_{k_B}}{\Delta W_{k_A} - 0.5\ \Delta W_{g_A}} < 1 \tag{39}$$

for an antiformal stack.

A forward-dipping duplex would be favored if

$$\frac{\Delta W_{p_B} + \Delta W_{k_B}}{\Delta W_{k_A} - 0.5\ \Delta W_{g_A}} > 1. \tag{40}$$

ESTIMATES OF WORK TERMS

The work terms used in the above analysis can be roughly quantified from field data to gain some understanding of the conditions under which the different duplex types may form. Similar estimates for energies involved in growth of and movement on large thrust faults were previously made by Elliott (1976b), using the McConnell thrust in the Canadian Rockies as an example. Wiltschko (1979b) also used energy estimates to determine the partitioning of forces in thrust sheet deformation for the Pine Mountain block in the Appalachians. Our estimates are based to some extent on Elliott's analysis, but take into account more recent work that we have done on thrust faults. The calculations are done for a near-surface duplex with fault spacing $s \simeq 5$ km involving a stratigraphic section of 2–4 km.

(a) *Nucleation of a thrust surface*

Under semi-brittle to ductile conditions the nucleation of cracks in grains is dislocation controlled (Lawn & Wilshaw 1975). These cracks usually grow in adjoining grains and eventually coalesce to form a fracture. The stresses necessary for crack nucleation can be represented by the Hall–Petch relation

$$\sigma_n = \sigma_o + \lambda D^{-1/2}, \tag{41}$$

where D is the average grain size of the rock; λ is an unpinning constant for dislocations given by

$$\lambda = \frac{\pi\sqrt{3}}{8}\left(\frac{8S_e\mu D}{\pi(1-\nu)L}\right)^{1/2}, \tag{42}$$

where S_e is the surface energy per unit area, μ is the shear modulus, ν is Poisson's ratio and L is the size of dislocation pile-ups within grains; and σ_o is the 'friction' stress resisting dislocation motion, given by

$$\sigma_o = \frac{2\mu}{K}\exp\left(\frac{-2\pi a}{K}\right) \tag{43}$$

where $K \simeq 1$ for edge dislocations, and a and b are spacings between atoms in two directions.

The crack is nucleated by a pile-up of n dislocations where

$$n = \frac{\pi L\sigma K}{\mu b} \simeq \frac{2L\sigma}{\mu b}. \tag{44}$$

Since crack nucleation occurs at 10^{-2}–10^{-3} of the theoretical strength, it requires a pile-up of 10^2–10^3 dislocations. The crack width is then given by

$$c = n \cdot b \simeq 10^3 \cdot b \text{ meters}. \tag{45}$$

b is typically 10^{-9} m for rock-forming minerals and hence $c = 10^{-6}$ m. The work required for a crack to nucleate is

$$W_n = \pi \cdot \frac{D^2}{4} \cdot \sigma_n \cdot c, \tag{46}$$

where σ_n is given by eqn (41). Typically, for rocks μ is 2×10^{10}–4×10^{10} Pa; theoretical estimates for S_e range from 0.1 to 1 Jm^{-2} for most materials (Paterson 1978) but rock forming minerals usually have S_e between 1 and 10 Jm^{-2} (e.g. quartz 0.4–1 Jm^{-2}, orthoclase 7.7 Jm^{-2}, Brace & Walsh 1962); Poisson's ratio (ν) for both sedimentary rocks and granitic basement rocks ranges from 0.2 to 0.4 (Birch 1966). Substituting these values into equation (46),

$$W_n = \pi \cdot \frac{D^2}{4} \cdot 10^{-6}(10^8 + 10^6 D^{-1/2}) \text{ J}$$

$$= \frac{\pi}{4}(D^2 \cdot 10^2 + D^{3/2}) \text{ J} \tag{47}$$

For typical grainsize, $D = 10^{-2}$–10^{-4} meters, W_n is negligibly small, particularly when it is compared to work involved in propagating a fracture.

(b) *Propagation of a thrust surface*

For a fault developed under ductile conditions of deformation, a bead of ductile rock exists along the tip line (Elliott 1976b). Rocks within this bead will deform so long as the long-term ductile yield strength of the rock is exceeded (Elliott 1976a). As the thrust propagates, this ductile bead sweeps out a volume of rock ahead of the propagating fracture. This entire volume of rock must have reached the finite strain necessary to induce ductile fracture. Assuming a simple shear deformation, the work W_p necessary to push this ductile zone ahead of a slice 1 km wide is

$$W_p = \tfrac{1}{8} \cdot \pi \cdot \tau_y \cdot \gamma_f \cdot a \cdot p \cdot 1000 \text{ J}, \tag{48}$$

where the long-term yield stress (τ_y) was estimated to be 2×10^7 Pa by Elliott (1976a). Other estimates of the differential stress in thrust sheets undergoing ductile deformation (based on dislocation densities, sub-grain-size and recrystallized grainsize) generally range from 10^7 to 10^8 Pa (see Schmid 1983). In metals undergoing plastic deformation, rupture occurs by necking when the work-hardening rate equals the effective stress (Anderson *et al.* 1974); the effective strain at necking is 0.1–0.3 (Anderson *et al.* 1974) corresponding to maximum shear strains (γ_f) of 0.2–0.6 (Ford & Alexander 1977). Equivalent plastic strains at fracture in torsion tests on metals are approximately 0.5 (McClintock & Argon 1966), although they may vary considerably depending on deformation conditions. Elliott (1976b) estimated γ_f at thrust tips in the Foothills and Front Ranges of the Canadian Rockies to range from 0.1 to 1, depending on the size and asymmetry of flexural slip folds preserved at the tips of thrusts of all sizes. Spratt (oral communication) determined both brittle and ductile strains at the tips of five thrusts that terminate in crinoidal and oolitic limestones in the Front Ranges of the Canadian Rockies. She found that natural octahedral unit shears (γ_{oct}) never exceed 1.4, corresponding to a maximum shear strain (γ_f) of 1.7 (Ford & Alexander 1977). Elliott (1976b) estimated the thickness of the deforming bead a to be ~1 km, and the down-dip length of the fault $p \simeq 5$ km for most duplexes (Boyer 1978). Using Elliott's stress estimate and assuming $\gamma_f \simeq 1.5$, we get

$$W_p \simeq 6 \times 10^{16} \text{ J}. \tag{49}$$

For faulting under brittle conditions, a similar ductile bead forms at the thrust tip (Irwin–Dugdale crack-tip models) where the rock yields due to stress concentrations at the crack tip (Ewalds & Wanhill 1984). In addition, the fault zone usually develops as a zone of close spaced fractures; major motion along the fault then takes place along this granulated zone. The work in propagating the fault thus involves work necessary to push the ductile bead ahead of the fault (similar to eqn 49), and work needed in granulating rock along the fault. For a slice of 1 km width, the latter is

$$W_p = \pi \cdot a_c \cdot p \cdot 1000 \cdot A_v \cdot S_c \text{ J}. \tag{50}$$

The down-dip length of the fault, $p \simeq 5$ km. The

thickness of the granulated zone (in a strain hardening situation) is $a_c \simeq 0.1u$ (Robertson 1983); the displacement (u) on a fault in a duplex may be up to 2.5 km (Boyer 1978) so that $a_c \simeq 0.25$ km. The surface area per unit volume $A_v \simeq 5 \times 10^2$ m^{-1} (Mitra 1980, in preparation). Surface energies (S_e) for rocks are generally orders of magnitude larger than those for single crystals; typical values are 10 Jm^{-2}, although they may range up to 100 Jm^{-2} (Paterson 1978). Substituting these values into eqn. (50)

$$W_p \simeq 1.9 \times 10^{13} \text{ J}. \quad (51)$$

(c) *Sliding on thrust surface*

Although the amount of sliding on the thrust is the same along either path in both the cases we have considered, it is instructive to evaluate the work involved in this process to compare it to the other work terms. Elliott (1976b) evaluated the sliding work assuming that it occurs on the thrust plane, a two-dimensional surface of zero thickness. For a slice that is 1 km in width, the work in sliding is

$$W_b = C \cdot \tau_b \cdot u \cdot p \cdot 1000 \text{ J}. \quad (52)$$

$C \simeq 1$ is a constant that accounts for the thrust gaining or losing displacement up and down the dip of the fault. The basal sliding stress was estimated to be 5×10^6 Pa by Elliott (1976b) for the McConnell thrust sheet in the Canadian Rockies. Stress–grainsize relations have been used to estimate fault-zone stresses as 10^6 Pa in the superplastic Lochseiten mylonite along the Glarus thrust in the Swiss Alps (Schmid, unpublished manuscript), and as 3×10^6 Pa in the cataclasites along the brittle White Rock thrust in the Wind River range of the Rocky Mountains (Mitra 1984). The down-dip length of the fault $p \simeq 5$ km for duplexes, and the displacement u may be up to 2.5 km for the faults in a duplex (Boyer 1978). From these values,

$$W_b \simeq 5 \times 10^{16} \text{ J}. \quad (53)$$

(d) *Work against gravity*

The work performed against gravity to emplace an imbricate slice of width 1 km is

$$W_g = \rho \cdot A \cdot h \cdot g \cdot 1000 \text{ J}. \quad (54)$$

The average density (ρ) of near surface rocks is 2.85×10^3 kg m^{-3} and the acceleration due to gravity g is 9.8 m s^{-2}. The height, h, that the excess cross-sectional mass is raised against gravity is equal to the depth to the lower glide horizon which we have chosen to be ~5 km (Fig. 11), but may vary considerably in individual duplexes. The cross-sectional area of the mass moved against gravity varies from one situation to another.

For Case I, cross-section area $A \simeq 2.5 \times 10^6$ m^2, and hence,

$$\Delta W_{g_B} \simeq 3.5 \times 10^{17} \text{ J}. \quad (55)$$

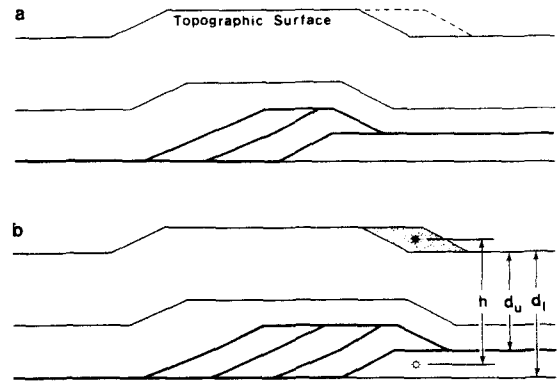

Fig. 11. Gravitational work performed by formation of and movement on a new imbricate fault. (a) Topographic surface above duplex having two imbricates. (b) The addition of a new imbricate alters the surface. The stippled area is the material added to the surface. h is the height through which the mass is raised against gravity, d_l is the depth of the lower glide horizon, and d_u is the depth of the upper glide horizon. For discussion, see text.

For a stack, $h \simeq 6$ km and

$$\Delta W_{g_A} \simeq 4.2 \times 10^{17} \text{ J}. \quad (56)$$

If, on the other hand, we consider a duplex forming at the erosional surface,

$$\Delta W_{g_A} = 2\,\Delta W_{g_B} = 1.3 \times 10^{17} \text{ J}. \quad (57)$$

In Case II, considerably more mass is moved. For path A, cross-sectional area $A \simeq 3.75 \times 10^6$ m^2, for path B, $A \simeq 3.25 \times 10^6$ m^2. For a lower glide horizon at a depth of 5 km the mass is raised approximately 5.5 km along path A and

$$\Delta W_{g_A} \simeq 5.75 \times 10^{17} \text{ J}. \quad (58)$$

The mass is raised approximately 6.5 km along path B and

$$\Delta W_{g_B} \simeq 6.3 \times 10^{17} \text{ J}. \quad (59)$$

If, on the other hand, we consider a duplex forming at the erosional surface,

$$\Delta W_{g_B} \simeq 1.5\,\Delta W_{g_A} \simeq 2.3 \times 10^{17} \text{ J}. \quad (60)$$

(e) *Internal deformation of imbricates*

The work done in internal deformation of the imbricates is more difficult to estimate than the other work terms. Although different deformation mechanisms may be operating depending on the metamorphic conditions under which the rocks are deforming (Elliott 1976b), and the detailed geometries of structures in the thrust sheet may be quite complicated, on a gross scale much of the work goes toward two main processes: flexural-slip folding within the sheet, and simple shear of the sheet which is generally concentrated toward the bottom of the sheet. It is not possible to model exactly the complicated internal geometry of a thrust sheet, and any estimates of the internal deformation work term will be only as good as the model used. In order to simplify the calculations, we have estimated the work involved in folding by using a simple kink-folding model. More

detailed analyses of the bending of a thrust sheet at a ramp have been published by Wiltschko (1979a). We have calculated the work involved in the overall simple shear of the sheet assuming that the sheet is perfectly plastic, so that overall simple shear within the sheet is confined to a basal layer. Even though this basal layer may be made up of thin deformation zones along which much of the slip is concentrated, the simple shear can be integrated over the entire basal layer without changing the results.

For the simplest duplex geometry (i.e., a hinterland-dipping duplex) each imbricate sheet can be subdivided into segments that have passed through a certain number of kink planes. Assuming a cross-sectional slice that is 1 km wide, the work in kinking each imbricate sheet is

$$\Delta W_k = \tau_{12} \sum_{i=1}^{n} \left(A_i \sum_{j=1}^{p} \tan \theta_j \right). \quad (61)$$

For an entire duplex made up of m horses,

$$W_k = \sum_{1}^{m} \left[\tau_{12} \sum_{i=1}^{n} \left(A_i \sum_{j=1}^{p} \tan \theta_j \right) \right], \quad (62)$$

where the long-term yield strength of the sheet gives $\tau_{12} = 2 \times 10^7$ Pa (Elliott 1976a). If we choose a ramp angle of 30°, the rocks are kinked through $\theta = 30°$ at each kink plane. For a duplex made up of three horses we find

$$W_k = 1.5 \times 10^{17} \text{ J}. \quad (63)$$

The average work per imbricate fault is then 5×10^{16} J. For a duplex made up of four horses,

$$W_k = 2.1 \times 10^{17} \text{ J}. \quad (64)$$

The work per imbricate is then 5.2×10^{16} J. Hence, as the duplex grows, the average work per slice increases.

Internal deformation by folding is most intense and complicated in the case of an antiformal stack. For a stack with four horses, the total work is

$$W_k = 4.2 \times 10^{17} \text{ J}. \quad (65)$$

The work per imbricate sheet is 1.05×10^{17} J. For a stack with three horses,

$$W_k = 3.44 \times 10^{17} \text{ J}. \quad (66)$$

The work per sheet is 1.5×10^{17} J. These work terms are approximately twice as large as those for hindward-dipping duplexes. Generally, the folding work terms are comparable to the overall simple shear term.

The overall simple shear within the sheet can be modelled as homogeneous simple shear within a basal layer whose thickness is approximately 0.1 of the displacement along the fault (Robertson 1983, Mitra 1979). Assuming a cross-sectional slice that is 1 km wide for each imbricate fault,

$$\Delta W_s = \tau_b \cdot \frac{u}{t_b} \cdot p \cdot t_b \cdot 1000 \text{ J}. \quad (67)$$

For an imbricate fault within a typical duplex the down-dip fault length (p) is 5 km and the displacement (u) is 2.5 km (Boyer 1978). For a weak basal zone τ_b is the same as the strength of the basal layer ($\sim 5 \times 10^6$ Pa) giving

$$W_s \simeq 6.25 \times 10^{16} \text{ J}. \quad (68)$$

For a strain softening basal layer τ_b must be the same as the long-term yield stress ($\tau_y \simeq 2 \times 10^7$ Pa) at the start of deformation, but may decrease as deformation progresses. Hence the simple-shear work may be as high as

$$W_s \simeq 2.5 \times 10^{17} \text{ J}. \quad (69)$$

Thus the average total internal work per imbricate sheet in a duplex is approximately 3×10^{17} J. This is probably a gross underestimate, considering our simplified model for internal deformation within the sheet. Elliott (1976b) estimated the internal work within the body of the McConnell thrust sheet, which is displaced 40 km, to be 6.4×10^{19} J. His estimate was based on the difference between external work provided and internal work expended within the system. To achieve the same displacement as the McConnell thrust along a duplex zone our model would require the development of 16 horses, and a total internal work of approximately 0.5×10^{19} J. This is certainly close to Elliott's estimate, considering the two estimates were made using totally different approaches. The correct answer may lie somewhere between these two estimates.

DISCUSSION AND CONCLUSIONS

Estimates of the work terms indicate that apart from fracture nucleation work (which is negligible compared to the other work terms), the work terms involved in duplex development are within two orders of magnitude of one another. Since individual work terms depend on material properties of the rocks (such as long-term yield stress τ_y, surface energy S_e, basal sliding stress τ_b and density ρ), the relative magnitudes of the work terms may change depending on variations in material properties of the rocks. Such variations in material properties may take place as a result of facies changes parallel or perpendicular to strike of a thrust belt. Alternatively, changes in metamorphic conditions during progressive deformation may cause changes in the material properties. The dominant deformation mechanism may also change during progressive deformation as grainsize or mineral assemblage changes along a fault zone.

The estimated work terms may be substituted into the two special transitional cases considered earlier in this paper. For Case I, the transition from hinterland-dipping duplex to antiformal stack, it is found that

$$\frac{\Delta W_{p_B} - \Delta W_{g_B}}{\Delta W_{k_A} - \Delta W_{k_B}} \simeq 1.4 \times 10^{-1} \ll 1.$$

This suggests that generally a hinterland-dipping duplex is favored energetically; it is also the type of duplex that is most commonly found. If movement on the faults is large (for example, if the fault is in an easy glide horizon and accumulates large displacements) the branch lines may coincide. We then have to consider Case II, the

transition from antiformal stack to foreland-dipping duplex; for this case, it is found that

$$\frac{\Delta W_{p_B} + \Delta W_{k_B}}{\Delta W_{k_A} - 0.5\,\Delta W_{g_A}} \simeq 1.5.$$

This suggests that slight variations in work terms may give rise to either an antiformal stack or a forward-dipping duplex.

This analysis of duplex development is based on the simplest duplex geometries and fairly simple-minded duplex development histories. It could, of course, be extended to more complicated geometries and to more realistic geologic situations, if more reliable data on geologic history, geometry and material properties were available.

Acknowledgements—This paper is based partly on a Ph.D. thesis (Boyer 1978). During his Ph.D. research SEB was supported by a National Science Foundation grant DES74-17647 to D. Elliott, and by grants from the Geological Society of America, Sigma Xi and the Johns Hopkins University Balk Fund. GM thanks J. Massare and G. Protzman for their help with the manuscript and illustrations, and the structure students at the University of Rochester for their comments. We thank the reviewers D. Wiltschko and E. G. Bombolakis; the latter's detailed comments were particularly useful in clarifying some parts of the paper. We both acknowledge our debt to our friend and advisor, the late David Elliott, whose many ideas we have drawn on in this paper.

REFERENCES

Anderson, J. C., Lever, K. D., Alexander, J. M. & Rawlings, R. D. 1974. *Materials Science* (2nd edn). Van Nostrand Reinhold (UK), Wokingham, England.

Birch, F. 1966. Compressibility, elastic constants. In *Handbook of Physical Constants* (edited by Clark, S. P., Jr.). *Mem. geol. Soc. Am.* **97**, 97–194.

Boyer, S. E. 1978. Structure and origin of Grandfather Mountain window, North Carolina. Ph.D. thesis, Johns Hopkins University.

Boyer, S. E. & Elliott, D. 1982. Thrust systems. *Bull. Am. Ass. Petrol Geol.* **66**, 1196–1230.

Brace, W. F. & Walsh, J. B. 1962. Some direct measurements of the surface energy of quartz and orthoclase. *Am. Miner.* **47**, 1111–1122.

Coward, M. P. 1984. The strain and textural history of thin-skinned tectonite zones: examples from the Assynt region of the Moine thrust zone, NW Scotland. *J. Struct. Geol.* **6**, 89–99.

Diegel, F. A. 1986. Topologic constraints on imbricate thrust networks—examples from the Mountain City window, Tennessee. *J. Struct. Geol.* **8**, 269–279.

Elliott, D. 1976a. The motion of thrust sheets. *J. geophys. Res.* **81**, 949–963.

Elliott, D. 1976b. Energy balance and deformation mechanisms of thrust sheets. *Phil. Trans. R. Soc. Lond.* **A283**, 289–312.

Elliott, D. & Johnson, M. R. W. 1980. Structural evolution in the northern part of the Moine thrust belt, NW Scotland. *Trans. R. Soc. Edinb., Earth Sci.* **71**, 69–96.

Ewalds, H. L. & Wanhill, R. J. H. 1984. *Fracture Mechanics*. Edward Arnold, London.

Fermor, P. R. & Price, R. A. 1976. Imbricate structures in the Lewis thrust sheet around Cate Creek and Haig Brook windows, southeast British Columbia. *Prof. Pap. Geol. Surv. Can.* **76-1B**, 7–10.

Ford, H. & Alexander, J. M. 1977. *Advanced Mechanics of Materials* (2nd edn). Halstead Press/John Wiley, New York.

Gilotti, J. A. & Kumpulainen, R. 1986. Strain-softening induced ductile flow in the Särv thrust sheet, Scandinavian Caledonides: a description. *J. Struct. Geol.* **8**, 441–455.

Gretener, P. E. 1972. Thoughts on overthrust faulting in a layered sequence. *Bull. Can. Petrol. Geol.* **20**, 583–607.

Hossack, J. R. 1983. A cross-section through the Scandinavian Caledonides constructed with the aid of branch-line maps. *J. Struct. Geol.* **5**, 103–111.

Lawn, B. R. & Wilshaw, T. R. 1975. *Fracture of Brittle Solids*. Cambridge University Press, Cambridge, England.

Martin, J. B. 1975. *Plasticity: Fundamentals and General Results*. MIT Press, Cambridge, Mass.

McClintock, F. A. & Argon, A. S. 1966. *Mechanical Behaviour of Materials*. Addison-Wesley, Reading, Mass.

Mitra, G. 1978. Ductile deformation zones and mylonites: the mechanical processes involved in the deformation of crystalline basement rocks. *Am. J. Sci.* **278**, 1057–1084.

Mitra, G. 1979. Ductile deformation zones in Blue Ridge basement rocks and estimation of finite strains. *Bull. geol. Soc. Am.* Pt. I. **90**, 935–951.

Mitra, G. 1980. Brittle and ductile deformation zones in granitic basement rocks of the Wind River mountains, Wyoming: a look at the brittle–ductile transition. *Geol. Soc. Am. Progr. with Abs.* **12**, 485.

Mitra, G. 1984. Brittle to ductile transition due to large strains along the White Rock thrust, Wind River Mountains, Wyoming. *J. Struct. Geol.* **6**, 51–61.

Nadai, A. L. 1963. *Theory of Flow and Fracture of Solids*, Volume 2. McGraw-Hill, New York.

Paterson, M. S. 1978. *Experimental Rock Deformation: The Brittle Field*. Springer, New York.

Robertson, E. C. 1982. Continuous formation of gouge and breccia during fault displacement. In *Issues in Rock Mechanics* (edited by Goodman, R. E. and Heuze, F. E.), Proc. 23rd Symp. on Rock Mechanics, *Am. Inst. Min. Engng*, 397–404.

Robertson, E . C. 1983. Relationship of fault displacement to gouge and breccia thickness. *Min. Engng*, 1426–1432.

Schmid, S. M. 1983. Microfabric studies as indicators of deformation mechanisms and flow laws operative in mountain building. In *Mountain Building Process* (edited by Hsu, K. J.), Academic Press, 95–110.

Suppe, J. 1983. Geometry and kinematics of fault-bend folding. *Am. J. Sci.* **283**, 684–721.

Wiltschko, D. V. 1979a. A mechanical model for thrust sheet deformation at a ramp. *J. geophys. Res.* **84**, 1091–1104.

Wiltschko, D. V. 1979b. Partitioning of energy in a thrust sheet and implications concerning driving forces. *J. geophys. Res.* **84**, 6050–6058.

Wojtal, S. W. 1982. Finite deformation in thrust sheets and their material properties. Ph.D. thesis, Johns Hopkins University.

APPENDIX

Work involved in kinking a thrust sheet at a ramp

Consider a single thrust-sheet climbing section through a competent unit. The thrust is assumed to be parallel to bedding in the lower and upper flats. A standing kind-band is set up in the area overlying the footwall ramp (Fig. 8). The advancing thrust sheet must pass through this kink-band, first being kinked at an angle equal to the ramp slope and then being kinked back to the horizontal at the top of the step. Thus, the material on the upper flat is kinked twice, while the material on the lower flat has not been kinked; inclined bedding overlying the ramp has been kinked only once. Assuming kink folding and its attendant flexural slip to be the dominant deformation processes, the work consumed can be estimated.

Figure 12(a) shows a section of flat-lying bedding (of length l_o, and thickness t) about to enter the kink plane at a ramp where the ramp angle is θ. The kink plane bisects the obtuse angle between bedding and the footwall ramp, so that bedding thickness remains the same after kinking. After a portion of the rock mass has passed through the kink (Fig. 12b), bedding within the kink-band is inclined at an angle θ. Strain within the kink-band is assumed to occur by bedding-plane slip and is calculated as follows.

Along the upper bedding surface

$$AB + BC + CD = l_o. \quad (1)$$

Along the lower bedding surface

$$EF + FG + GH + HJ = l_o. \quad (2)$$

Since AB = EF and BC = HJ

$$CD = FG + GH = d. \quad (3)$$

This is the distance that the upper bedding surface moves forward with respect to the lower bedding surface, resulting in rotation of DJ (a

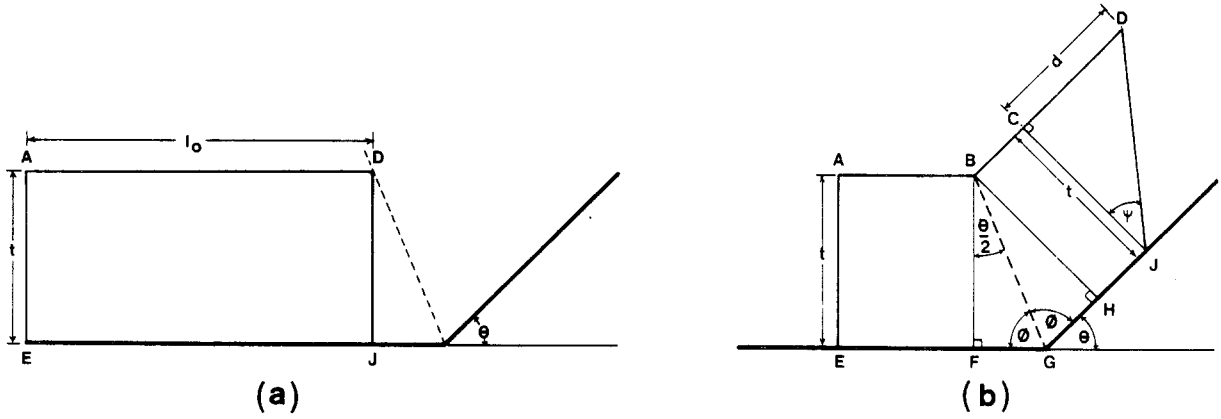

Fig. 12. (a) A section of flat-lying bedding, of length l_o and thickness t about to enter the kink plane at a ramp with ramp-angle θ. (b) After a portion of bedding has passed through the kink plane, the bedding within the kink band is inclined at angle θ. The bedding makes an angle $\phi = 90 - \theta/2$ with the kink plane. The upper bedding surface has moved forward through a distance d with respect to the lower bedding surface.

line originally perpendicular to bedding) through an angle ψ. The shear strain γ is then given by

$$\gamma = \frac{d}{t} = \tan \psi. \tag{4}$$

The angle (ϕ) between bedding and the kink plane is given by

$$\phi = \frac{180 - \theta}{2} = 90 - \frac{\theta}{2}. \tag{5}$$

$$\hat{FBG} = \hat{GBH} = \frac{\theta}{2} \tag{6}$$

and

$$FG = GH = t \tan\left(\frac{\theta}{2}\right). \tag{7}$$

From (3) and (7)

$$d = 2t \tan\left(\frac{\theta}{2}\right). \tag{8}$$

From (4) and (8)

$$\gamma = \tan \psi = 2 \tan\left(\frac{\theta}{2}\right). \tag{9}$$

or

$$\psi = \tan^{-1}\left[2 \tan\left(\frac{\theta}{2}\right)\right]. \tag{10}$$

For most thrust faults $\theta \leq 30°$ and for these angles,

$$\frac{\psi}{\theta} > 0.9. \tag{11}$$

Substituting in (4),

$$\gamma \simeq \tan \theta. \tag{12}$$

The work per unit volume is given by

$$W = \tau_{12} \cdot \gamma \simeq \tau_{12} \cdot \tan \theta. \tag{13}$$

The work in kinking a slice of cross-sectional area A and unit width parallel to strike within the kink band overlying the footwall ramp is given by

$$W_{k1} = \tau_{12} \cdot \tan \theta \cdot A \cdot 1. \tag{14}$$

The material in the upper flat (Fig. 8) has gone through two kink planes, at each one of which it is bent through an angle θ. The work done on this material is

$$W_{k2} = 2 \cdot \tau_{12} \cdot \tan \theta \cdot A_2 \cdot 1. \tag{15}$$

Therefore, for the entire thrust sheet, work done in kinking is

$$W_k = W_{k1} + W_{k2} = \tau_{12} \cdot \tan \theta \cdot A_1 + 2\tau_{12} \cdot \tan \theta \cdot A_2 \tag{16}$$

In the most general case, the bending angles θ at successive kink planes are not necessarily the same, and hence,

$$W_k = \tau_{12} \cdot A_1 \cdot \tan \theta_1 + \tau_{12} \cdot A_2(\tan \theta_1 + \tan \theta_2), \tag{17}$$

or

$$W_k = \tau_{12} \sum_{i=1}^{n} \left(A_i \sum_{j=1}^{p} \tan \theta_j\right). \tag{18}$$

In a duplex, each imbricate thrust sheet (horse) is kinked as it is emplaced. In addition, parts of each horse are unkinked or kinked again when succeeding horses are emplaced. The mass within each horse can be divided into subareas (n), based on the number of kink planes (p) each volume of rock has passed through. The total work for m horses is

$$W_k = \sum_{1}^{m} \tau_{12}[A_1(\tan \theta_1 + \cdots + \tan \theta_p) + \cdots + A_n(\tan \theta_1 + \cdots + \tan \theta_p)], \tag{19}$$

or,

$$W_k = \sum_{1}^{m} \left[\tau_{12} \cdot \sum_{i=1}^{n} \left(A_i \cdot \sum_{j=1}^{p} \tan \theta_j\right)\right]. \tag{20}$$